Future Engineering Journal

Volume 2 | Issue 1 Article 4

January 2021

Optimal Nonlinear PID Speed Control Based on Harmony Search for An Electric Vehicle

Mohamed Shamseldin
Future University in Egypt, mohamed.abelbbar@fue.edu.eg

Mohamed Abdel Ghany
6 October University, mghany1988@hotmail.com

Yahia Hendawey
Future University in Egypt, Yahia.Hendawey@fue.edu.eg

Optimal Nonlinear PID Speed Control Based on Harmony Search for An Electric Vehicle

Cover Page Footnote

We would like to express our deepest thanks to the Future University in Egypt.

FUTURE ENGINEERING JOURNAL 2 (2021) 2314-7237

HOSTED BY

ELSEVIER

Future Engineering Journal

Journal homepage: http://digitalcommons.aaru.edu.jo/fej/

Optimal Nonlinear PID Speed Control Based on Harmony Search for An Electric Vehicle

Mohamed. A. Shamseldin[a*], M. A. Abdel Ghany[b], Yehia . H. Hossamel-din[c]

[a] *Mechanical Engineering Department, Future University in Egypt (FUE), Cairo, Egypt*

[b]*Electrical Engineering Department, 6 October University, Cairo, Egypt*

[c]*Chairman, Mech. Eng. Dept., Future University in Egypt (FUE), Cairo, Egypt*

ARTICLEINFO

Article history
Received **August 2020**
Accepted **November 2020**

Keywords:
Electric Vehicle (EV)
Harmony Search (HS)
PID
Nonlinear PID (NPID)

ABSTRACT

The paper presents an efficient scheme for a Nonlinear PID (NPID) controller to improve the dynamic response of the Electric Vehicle (EV). The objective of the proposed controller is to track accurately the reference speed selected by the driver of the EV. A MATLAB/Simulink model is established and validated for the considered EV to study the system performance. The proposed NPID controller has been investigated by comparing it with the traditional PID controller. The optimal parameters of Both the NPID and PID controllers were obtained using the Harmony Search (HS) optimization technique based on a cost function. The desired rise time, settling time, steady-state error, and overshoot have been taken into account in the cost function. Two tests were performed, the first test was implemented at fixed reference speed while the second one was carried out at a staircase command of reference speed. The simulation results can be summarized as follows: in the first test, the NPID controller reaches the steady-state speed at 38.12 seconds while the PID controller stabilizes at 44.68 seconds. Moreover, the NPID controller has a 0.5% steady-state error however, the PID controller has a 4% steady-state error. Besides, the second test shows that the NPID controller can decrease the root mean square of error by 30.1% compared to the PID controller. Lastly, the proposed NPID controller can enhance EV performance significantly.

1. Introduction

In recent years, several countries and global organizations seek to enhance the use of Electrical Vehicles (EV). This is to overcome the pollution problems and to decrease the dependence on petroleum fuel energy (Franchi and Mallet 2017). However, due to the high cost and short lifetime of batteries, the EV has just 0.02 % of the global vehicles by the end of 2012 (Gong, Liu, and Tang 2013). Nowadays, batteries manufacturing technology has been developed to get a longer life period and faster charge time (Zhu et al. 2012).

There is a considerable wealth in the literature having the EV models (As examples: references (Gaurav and Gaur 2020), (Dinc and Otkur 2020)). Usually; The complexity of the model depends on the required accuracy and the parameters needed to be studied. The model presented in this study has been developed to be simple enough to save execution time and memory space and at the same time it is complicated enough for studying accurately the behavior of the needed parameters.

* *Corresponding author.* Tel.: +2-01098807058; fax: +202 26186111.
E-mail address: mohamed.abelbbar@fue.edu.eg

Peer review under responsibility of Faculty of Engineering and Technology, Future University in Egypt.

http://digitalcommons.aaru.edu.jo/fej/

The EV system can split into two main subsystems: the first subsystem presents the mechanical transmission and wheels (Stankovi et al. 2014), while the second represents the electric motor, battery, and speed controller (Press et al. 2013). The objective of the speed controller is to regulate the EV under a reference speed selected by the driver.

Several control techniques can be implemented for regulating the EV speed (Technology 2015): For example, the classical PID control which is used in various engineering applications (Mohamed A. Shamseldin, Sallam, Bassiuny, and Ghany 2019). The conventional PID control is suitable for linear and simple systems (Bingul 2018), but it gives a poor performance for most of the complicated nonlinear systems, and also, it is not valid through systems having different operating points (Aghdam et al. 2017).

More advanced control techniques can be used to overcome the mentioned problems of conventional PID control (M.A. Shamseldin, El-Samahy, and Ghany 2017). One of these techniques is fuzzy logic where it can solve the problems of nonlinearity and uncertainty (Mohamed A. Shamseldin et al. 2018). On the other hand, a fuzzy-logic control system needs previous experience for systems, which sometimes is not available. Also, it lacks sufficient capacity for the new rules (Hurtik, Molek, and Hula 2020).

Using neural-network in designing a control system has the advantage of a strong ability to solve the structured uncertainty and the disturbance of the system, but it requires more computing capacity and data storage space (Moore, Berger, and Song 2020), (Siegel 2020). Sliding mode (SM) control is suitable for nonlinear systems and has the advantages of having a fast response, unaffected by disorders, and variable operating points (Upadhya 2017), (Rajabi and Hossein 2018). The main disadvantage of SM control is the shuttering signal of controller output which leads to difficulties to implement it practically (Engineering and Issn 2017).

Generally, the EV is a complex nonlinear system, and accordingly using the classical PID controller may not give satisfactory results. This study presents an advanced proposed nonlinear PID (NPID) controller with nonlinear gains incorporated with the fixed gains of the classical PID controller (Ren, Li, and Zhang 2010). These nonlinear gains enjoy the advantage of high initial gain to attain a fast dynamic response, followed by a low gain to prevent an oscillatory behavior (Zheng, Su, and Mercorelli 2019). Many studies confirmed that the Harmony Search (HS) optimization technique can reach the optimum solution more efficiently compared to other optimization techniques(Pathak and Sengupta 2020).

The main contribution of this paper is the design and implementation of a new form of a nonlinear PID control for the speed of an EV. A validated EV model has been developed and a tuning system using the HS optimization technique is considered to obtain the optimal values for the controller parameters based on an effective cost function. A comparative study between the performance of the proposed NPID controller and that of the classical PID controller is also introduced.

The paper has been organized as follows: firstly, the simple electric vehicle model is presented. Secondly, the proposed control technique is demonstrated. Thirdly, the simulation results are illustrated. Finally, the conclusion is discussed.

Nomenclature

A	system matrix
B	input matrix
BW	bandwidth factor
HMCR	harmony memory consideration rate
HMS	harmony memory solution
J_1	vehicle inertia
J_m	motor inertia
K	spring constant for connection rotor
K_b	back EMF constant
K_i	integral gain
$K_{ni}(e)$	nonlinear vector gain (i=1,2,3)
K_t	torque constant
K_d	derivative gain
K_p	proportional gain
L_m	motor inductance
M_p	overshoot
PAR	pitch adjustment rate
R_m	motor resistance
S	linear vehicle displacement
b	spring damping for connection rotor
b_1	vehicle damping
r_1	gearing ratio between motor and tire - meters travelled per radian of motor rotation
t_s	rise time
u	the rated voltage
v	linear car velocity
w_1	*wheel rotational speed*
w_i	nonlinear constant gains (i=1,2,3)
w_m	rotational motor speed
x	state vector

β	weight factor
θ_1	wheel rotational displacement
θ_m	*motor rotational displacement*
τ	*Time constant of a lag between motor torque and car velocity*

2. The proposed electric vehicle model

This section demonstrates the mathematical model equations for EV. Fig. 1 shows the main components of the considered EV, which are: brushed DC motor, battery, speed controller, Mechanical transmission (gears), and tires. Table 1 shows the parameters and their values for this EV. Besides, Fig. 2 illustrates its free body diagram.

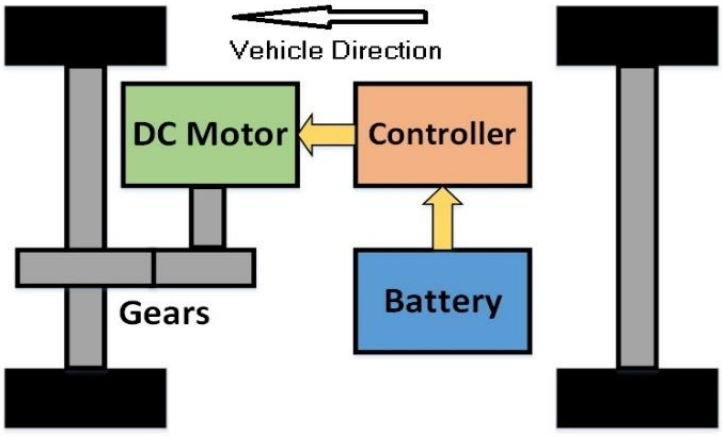

Fig. 1 - Block diagram of electric vehicle main components.

Table 1- Electric vehicle parameters.

No.			**DC motor parameters**
1	R_m	0.1	Motor resistance (ohm)
2	L_m	0.01	Motor inductance (Henrys)
3	K_b	6.5*10^-4	Back EMF constant (Volt-sec/Rad)
4	K_t	0.1	Torque constant (Nm/A)
5	J_m	1.0*10^-4	Rotor inertia (Kg.m2)
6	b_m	1.0*10^-5	Mechanical damping (linear model of friction)
7	u	36	The rated voltage (V)
No.			**Automobile parameters**
1	J_1	1000 * J_m	Vehicle inertia (1000 times the rotor) (Kg.m2)
2	b_1	1.0*10^-3	Vehicle damping (friction)- (N.m/(rad/s))
3	K	1.0*10^2	Spring constant for connection rotor/drive shaft (N/m)
4	b	0.1	Spring damping for connection rotor/drive shaft (N.m/(rad/s))
5	r_1	0.005	Gearing ratio between motor and tire - meters travelled per radian of motor rotation (m/rad)
6	τ	2	The time constant of a lag between motor torque and car velocity. This lag is a simplified model of the power train. (sec)

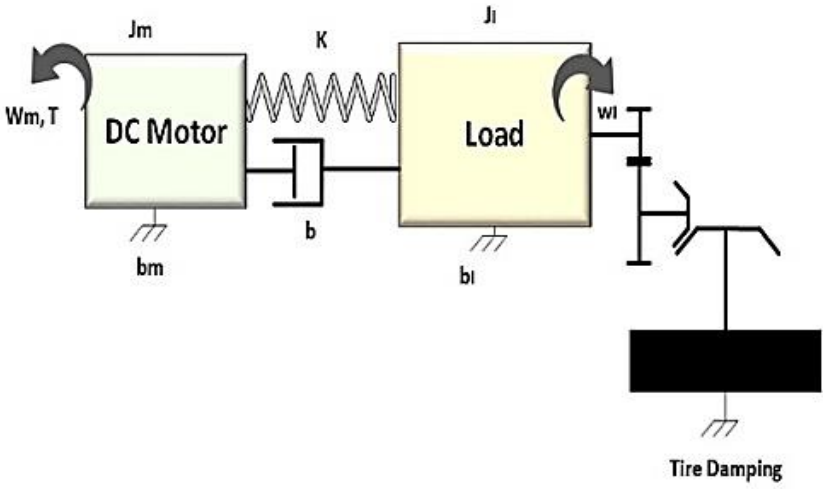

Fig. 2 - Free body diagram of EV.

The equations representing this EV dynamics and state-space model can be summarized as follows:
Firstly, the motor electrical circuit.

$$u = L_m \frac{di}{dt} + R_m i + K_b w_m \tag{1}$$

$$\frac{di}{dt} = \frac{-R_m}{L_m} i - \frac{K_b}{L_m} w_m + \frac{u}{L_m} \tag{2}$$

Secondly, the dynamics of the motor shaft.

$$J_m \frac{dw_m}{dt} = K_t i - w_m b_m - b(w_m - w_1) - K(\theta_m - \theta_1) \tag{3}$$

$$\frac{dw_m}{dt} = \frac{K_t}{J_m} i - \frac{(b_m + b)}{J_m} w_m - \frac{K}{J_m} \theta_m + \frac{b}{J_m} w_1 + \frac{K}{J_m} \theta_1 \tag{4}$$

$$\frac{d\theta_m}{dt} = w_m \tag{6}$$

Thirdly, the dynamics of the load.

$$J_1 \frac{dw_1}{dt} = b(w_m - w_1) + K(\theta_m - \theta_1) - b_1 w_1 \tag{7}$$

$$J_1 \frac{dw_1}{dt} = b w_m + K\theta_m - (b + b_1) w_1 - K\theta_1 \tag{8}$$

$$\frac{dw_1}{dt} = \frac{b}{J_1} w_m + \frac{K}{J_1} \theta_m - \frac{(b + b_1)}{J_1} w_1 - \frac{K}{J_1} \theta_1 \tag{9}$$

$$\frac{d\theta_1}{dt} = w_1 \tag{10}$$

Assume the relation between v and w_m has been presented as a first-order system given by:

$$\tau \frac{dv}{dt} + v = r_1 w_m \tag{11}$$

$$\frac{dv}{dt} = \frac{r_1}{\tau} w_1 - \frac{v}{\tau} \tag{12}$$

At steady state

$$r_1 = \frac{v}{w_1} \tag{13}$$

$$\frac{ds}{dt} = v \tag{14}$$

$$\dot{x} = A.x + B.u \tag{15}$$

$$A = \begin{bmatrix} \frac{-R_m}{L_m} & \frac{-K_b}{L_m} & 0 & 0 & 0 & 0 & 0 \\ \frac{K_t}{J_m} & \frac{-(b_m+b)}{J_m} & \frac{-K}{J_m} & \frac{b}{J_m} & \frac{K}{J_m} & 0 & 0 \\ 0 & 1 & 0 & 0 & 0 & 0 & 0 \\ 0 & \frac{b}{J_1} & \frac{K}{J_1} & \frac{-(b+b1)}{J_1} & \frac{-K}{J_1} & 0 & 0 \\ 0 & 0 & 0 & 1 & 0 & 0 & 0 \\ 0 & 0 & 0 & \frac{r_1}{\tau} & 0 & \frac{-1}{\tau} & 0 \\ 0 & 0 & 0 & 0 & 0 & 1 & 0 \end{bmatrix} \quad (16)$$

$$B = \begin{bmatrix} \frac{1}{L_m} & 0 & 0 & 0 & 0 & 0 & 0 \end{bmatrix}^T \quad (17)$$

$$x = [i \quad d\theta_m \quad \theta_m \quad d\theta_1 \quad \theta_1 \quad v \quad s]^T \quad (18)$$

This open-loop EV model was built by John Hedengren and was considered by Mathworks (Hedengren 2007). In this paper, the EV model has been developed to a SIMULINK MATLAB file. The proposed SIMULINK model has been validated by comparing its results to Hedengren ones, which were identical. Also, this validated model has been used in combination with the proposed controllers to illustrate the enhancement of the performance of the considered EV.

The open-loop velocity response at the rated voltage has been obtained and shown in Fig. 3 shows. It can be noted that the vehicle velocity reaches 50 m/s (180 km/hr) through 150 seconds, which is a long speeding up time.

Fig. 4 demonstrates the corresponding rotor current of the DC motor. It is clear that the current increases to 180 A and then decreases to 115 A.

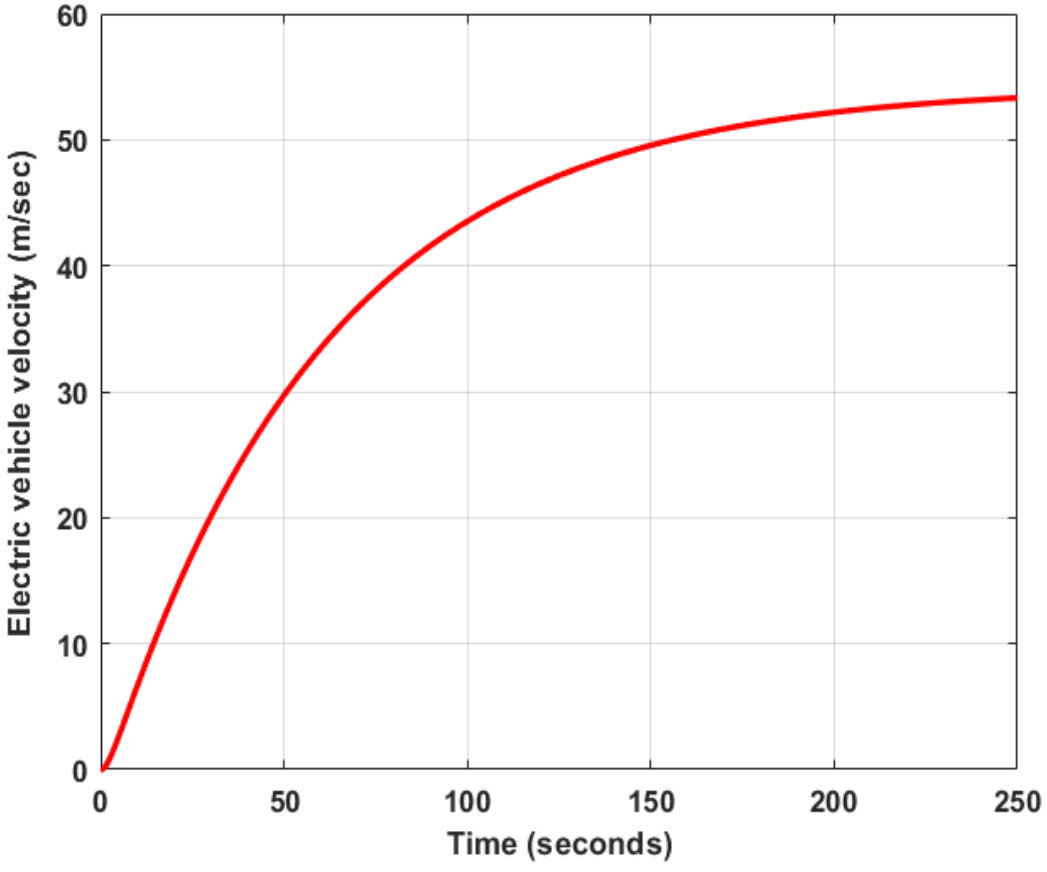

Fig. 3 - The open loop electric vehicle velocity response at rated voltage.

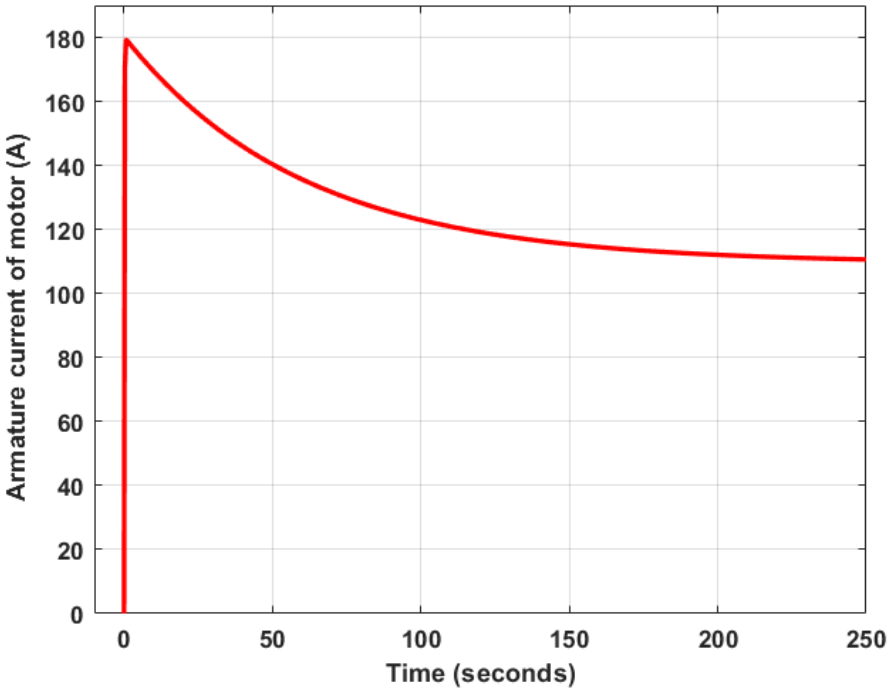

Fig. 4 - The corresponding rotor current at open-loop case.

3. Enhanced nonlinear PID controller

It is well known that the transfer function of the linear PID controller is $K(s) = K_P + K_i/s + K_d s$. Where K_p, K_i and K_d are fixed gains. These gains can be defined as follows. K_p is the proportional gain which attempts to reduce the error responses. K_i is the integral gain and its role is to eliminate the steady-state error. k_d is the differential gain which decreases the overshoot of the system and also, it improves the system stability (Scientiarum 2017), (Mohamed A Shamseldin, Eissa, and El-samahy 2015).

The linear fixed parameters PID controllers are often suitable for controlling a simple physical process but the demands for high-performance control with different operating point conditions or environmental parameters are often beyond the abilities of simple PID controllers (Abdel Ghany, Shamseldin, and Abdel Ghany 2017), (Zheng, Su, and Mercorelli 2019). The performance of linear PID controllers can be enhanced using several techniques that are being developed to deal with sudden disturbances and complex systems, for example, the PID self-tuning methods, neural networks, and fuzzy logic strategies, and other methods (Zhao and Ren 2016).

Among these techniques, nonlinear PID (NPID) control is presented as one of the most appropriate and effective methods for industrial applications. The nonlinear PID (NPID) control is carried out in two broad categories of applications. The first category is particular to nonlinear systems, where NPID control is used to absorb the nonlinearity. The second category deals with linear systems, where NPID control is used to obtain enhanced performance not realizable by a linear PID control, such as reduced overshoot, diminished rise time for a step or rapid command input, obtained better tracking accuracy and used to compensate the nonlinearity and disturbances in the system (M.A. Shamseldin, Ghany, and Ghany 2018), (Salim and Junoh 2017). The NPID controllers have the advantage of high initial gain to achieve a fast dynamic response, followed by a low gain to avoid unstable behavior. In this study, the traditional linear PID controller is enhanced by combining a sector-bounded nonlinear gain into a linear fixed gain PID control architecture.

The proposed enhanced nonlinear PID (NPID) controller consists of two parts. The first part is a sector bounded nonlinear gain $K_n(e)$ while the second part is a linear fixed-gain PID controller (K_p, K_i and K_d). The nonlinear gain $K_n(e)$ is a sector-bounded function of the error e(t). The previous researches have considered the nonlinear gain $K_n(e)$ as a one scalar value (M.A. Shamseldin, Ghany, and Ghany 2018).

In this research, the one scalar value of $K_n(e)$ will be replaced with a row vector which can be expressed as: $K_n(e) = [K_{n1}(e) \quad K_{n2}(e) \quad K_{n3}(e)]$, as shown in Fig. 5. This will lead to improving the performance of nonlinear PID controller where the values of nonlinear gains will be adjusted according to the error and the type of fixed parameters (K_p, K_i and K_d).

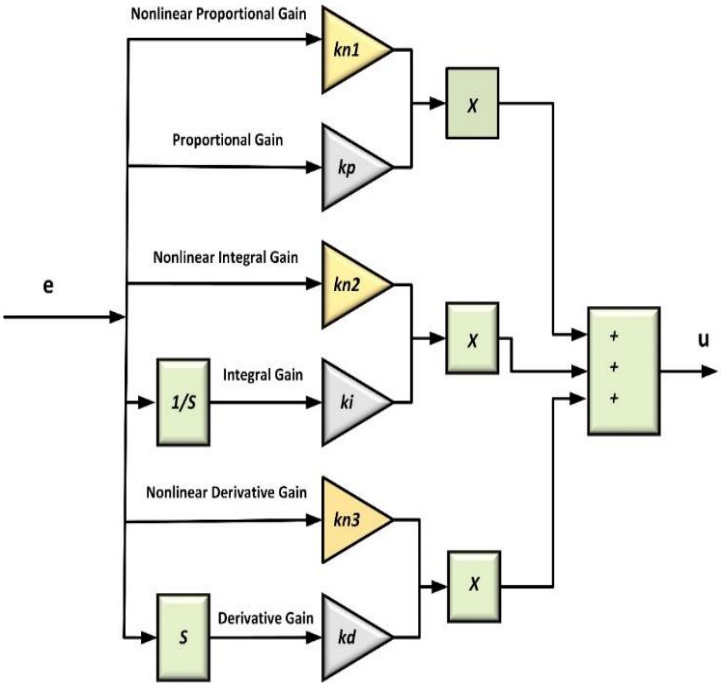

Fig. 5 - The NPID controller structure.

The proposed form of NPID control can be described as follows:

$$u(t) = K_p[K_{n1}(e).e(t)] + K_i \int_0^t [K_{n2}(e).e(t)]\,dt + K_d\left[K_{n3}(e).\frac{de(t)}{dt}\right] \quad (19)$$

Where $K_{n1}(e), K_{n2}(e)\ and\ K_{n3}(e)$ are nonlinear gains. The nonlinear gains represent any general nonlinear function of the error which is bounded in the sector $0 < K_n(e) \leq K_n(e)$max.

There is a wide range of choices available for the nonlinear gain $K_n(e)$. One simple form of the nonlinear gain function can be described as.

$$K_{ni}(e) = ch(w_i e) = \frac{\exp(w_i e)+\exp(-w_i e)}{2} \quad (20)$$

Where $i = 1, 2, 3$.

$$e = \begin{cases} e & |e| \leq e_{max} \\ e_{max} sgn(e) & |e| > e_{max} \end{cases} \quad (21)$$

The nonlinear gain $K_n(e)$ is lower bounded by $K_n(e)\min = 1$ when e = 0, and upper-bounded by $K_n(e)\max = \text{ch}(w_i\ e_{max})$. Therefore, e_{max} stand for the range of deviation, and w_i describes the range of variation of $K_n(e)$ and the degree of nonlinearity for each parameter.

The performance of the PID and NPID controllers are highly affected by the values of their parameters. There are different approaches to find the parameters of the PID controller, for instance, try and error and Ziegler-Nichols method but, most of these approaches do not usually give the best results. In this paper, the harmony search optimization technique will be used to obtain the optimal values of both PID and NPID controller parameters according to the objective function shown in Eq (22) (Mohamed A. Shamseldin, Sallam, Bassiuny, and Abdel Ghany 2019).

$$f = \frac{1}{(1-e^{-\beta})(M_p+e_{ss})+e^{-\beta}(t_s-t_r)} \quad (22)$$

Where e_{ss} is the steady-state error, M_p is the overshoot of system response, t_s is the settling time and t_r is the rise time. Also, this objective function is able to compromise the designer requirements using the weighting parameter value (β). The parameter is set larger than 0.7 to reduce overshoot and steady-state error. If this parameter is adjusting smaller than 0.7 the rise time and settling time will be reduced. Harmony search (HS) was suggested by Zong Woo Geem in 2001 (Ebrahim and Bendary 2016). It is well known that HS is a phenomenon-mimicking algorithm inspired by the improvisation process of musicians (Omar et al. 2016).

The initial population of Harmony Memory (HM) is chosen randomly. HM consists of Harmony Memory Solution (HMS) vectors. The HM is filled with HMS vectors as follows:

$$HM = \begin{bmatrix} K_{p\,(1,1)} & K_{i\,(1,2)} & K_{d\,(1,3)} & w_{1\,(1,4)} & w_{2\,(1,5)} & w_{3\,(1,6)} \\ K_{p\,(2,1)} & K_{i\,(22)} & K_{d\,(2,3)} & w_{1\,(2,4)} & w_{2\,(2,5)} & w_{3\,(2,6)} \\ . & . & . & . & . & . \\ . & . & . & . & . & . \\ . & . & . & . & . & . \\ K_{p\,(HMS,1)} & K_{i\,(HMS,2)} & K_{d\,(HMS,3)} & w_{1\,(HMS,4)} & w_{2\,(HMS,5)} & w_{3\,(HMS,6)} \end{bmatrix} \quad (23)$$

Harmony Memory Consideration (HMC) rule, for this rule a new number r1 is generated within the range [0 1]. If r1 <HMCR, where HMCR is the harmony memory consideration rate, then the first decision variable in the new vector x_{newij} is chosen randomly from the values in the current HM as follows (Pathak and Sengupta 2020):

$$x_{ij}^{new} = x_{ij},\ x_{ij} \in \{x_1, x_2, x_3, \dots\dots, x_{HMSJ}\} \quad (24)$$

The obtained decision variables from the harmony memory consideration rule are further examined to determine if it needs to pitch adjustment or not. A new random number r2 is generated within the range [0 1]. If r2 < PAR, where PAR is a pitch adjustment rate, then the pitch adjustment decision variable is calculated as follows:

$$x_{ij}^{new} = x_{ij} \pm rand(0,1).BW \quad (25)$$

where BW is a bandwidth factor, which is used to control the local search around the selected decision variable in the new vector. Random initialization rule, If the condition r1 < HMCR fails, the new first decision variable in the new vector x_{ij}^{new} is generated randomly as follows:

$$x_{ij}^{new} = l_{ij} + \left(u_{ij} - l_{ij}\right).rand(0,1) \quad (26)$$

where l,& u are the lower and upper bound for the given problem. After the harmony vector $x^{\{new\}}$ is generated, it will replace the worst harmony vector $x^{\{worst\}}$ in the harmony memory if its objective

function value is better than the objective function value of the worst harmony vector. Fig. 6 demonstrates the Harmony search tuning system flow chart.

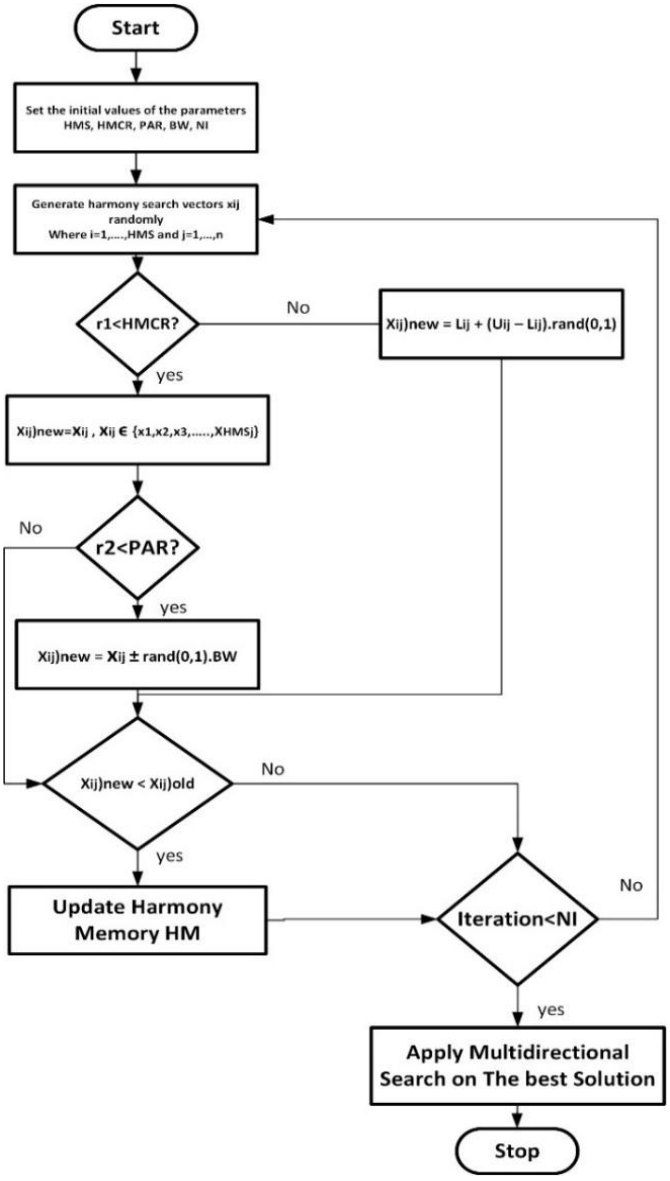

Fig. 6 - The harmony search flow chart.

The HS tuning system parameters and the search range of each controller parameters are demonstrated in Table 2. These ranges are selected based on Ziegler and Nichols method by increase and decrease the obtained value for each parameter.

Table 2. Harmony search tuning system parameters.

Technique	Parameters	Value
HS	HMCR	0.98
	PAR	0.3
	BW	0.01
PID controller	K_p	Range [0 – 50]
	K_i	Range [0 – 50]
	K_d	Range [0 – 50]
NPID controller	K_p	Range [0 – 50]
	w_1	Range [0 – 1]
	K_i	Range [0 – 50]
	w_2	Range [0 – 1]
	K_d	Range [0 – 50]
	w_3	Range [0 – 1]

Fig. 7 and Fig. 8 illustrate the convergence curve of the NPID controller parameters to optimal values through the HS tuning system.

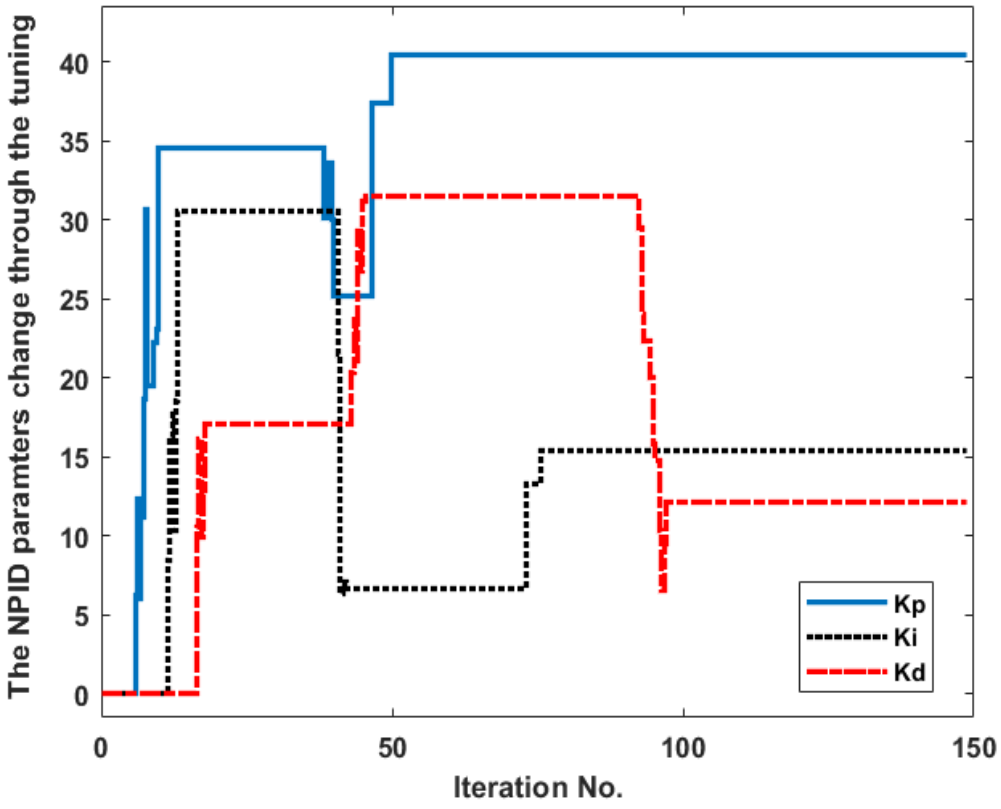

Fig. 7 - The change of K_p, K_i, and K_d through the HS tuning operation.

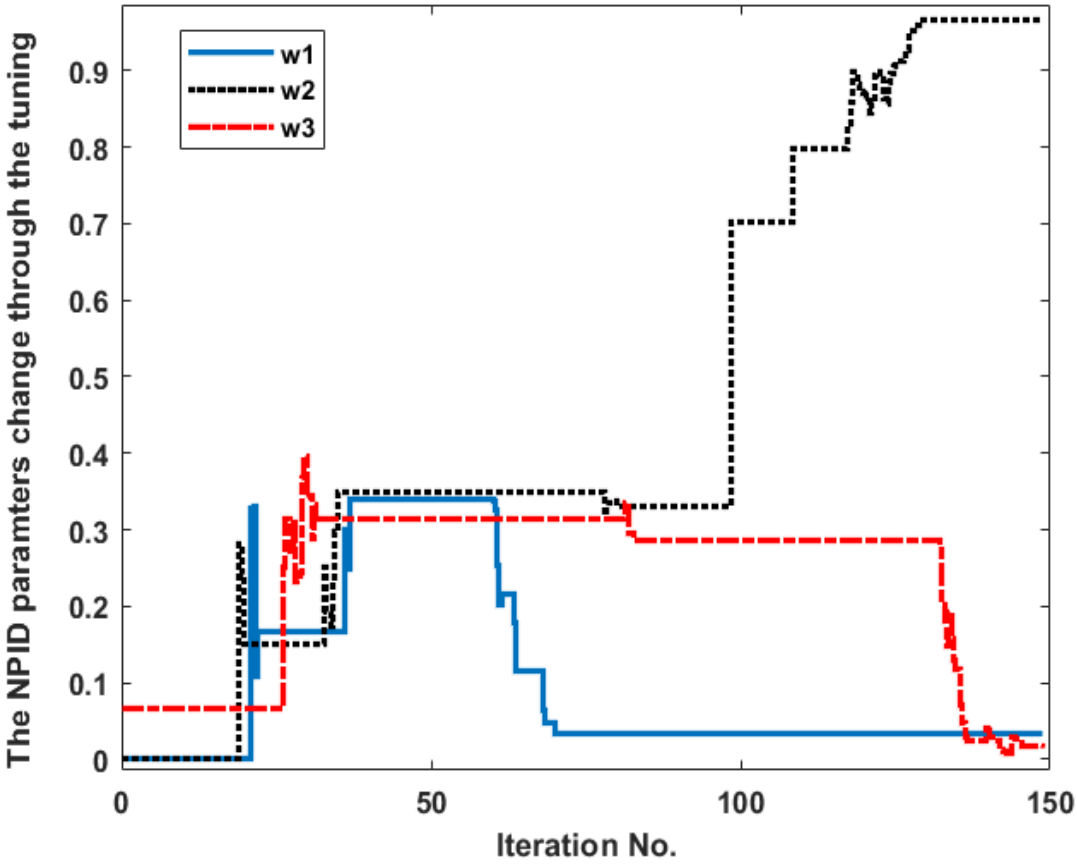

Fig. 8 - The EV velocity response at fixed reference speed.

Table 3 illustrates the obtained values of parameters through the optimization operation.

Table 3 - Optimal Controllers Parameters.

Controller Type	Controller parameters					
PID Controller	K_p		K_i		K_d	
	10		0.01		56	
NPID Controller	K_p	w_1	K_i	w_2	K_d	w_3
	40.5	0.01	15.05	0.96	11.034	0.04

4. Simulation results

This section demonstrates the EV performance using conventional PID control and the proposed control technique. Two tests will be implemented: in the first test, the driver adjusts the EV at a fixed reference speed while in the second test the driver will change the reference speed continuously. This is to investigate the robustness of the controller.

Fig. 9 shows the EV velocity response at a fixed reference speed in case of using PID & NPID. It can be noted that the NPID control has a faster response, smooth behavior, no overshoot, and zero steady-state error. The EV can reach the required speed in 14 seconds. In contrast to that, the PID control has a slow response and high steady-state error (6%).

Table 4 illustrates a detailed comparison between the NPID controller and the PID controller. It can be noted that the NPID controller reaches the steady-state speed at 38.12 seconds while the PID controller steadies at 44.68 seconds. Furthermore, the NPID controller has a 0.5% steady-state error however, the PID controller has a 4% steady-state error.
Fig. 10 demonstrates the corresponding armature current of the motor in both two controllers. Fig. 11 shows the traveled distance through the test. It is obvious that the EV with NPID control travels more than the conventional PID control.

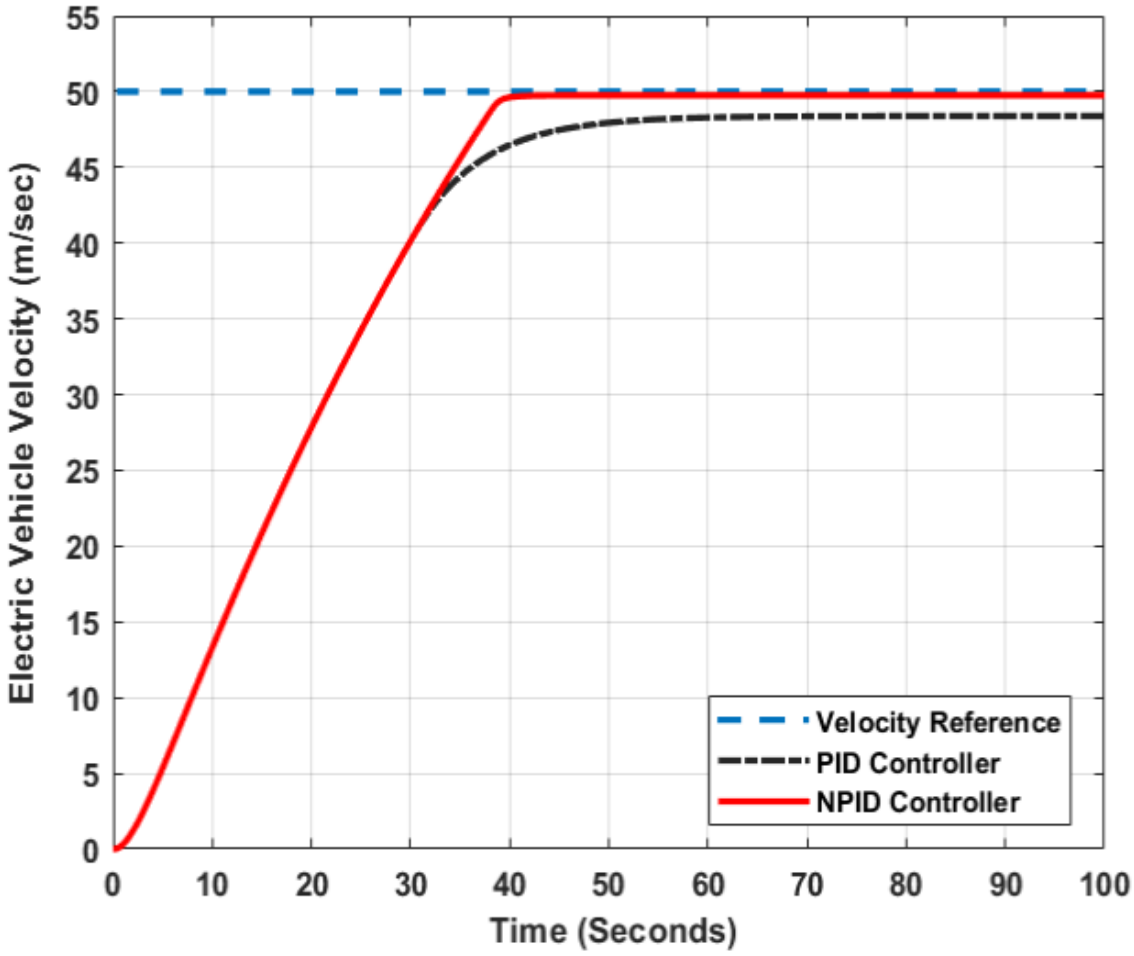

Fig. 9 - The EV velocity response at fixed reference speed.

Table 4 - The proposed controller's performance.

Performance	PID controller	NPID controller
t_r (s)	29.04	29.01
t_s(s)	44.87	38.12
e_{ss} (%)	4%	0.5%
M_p	0	0

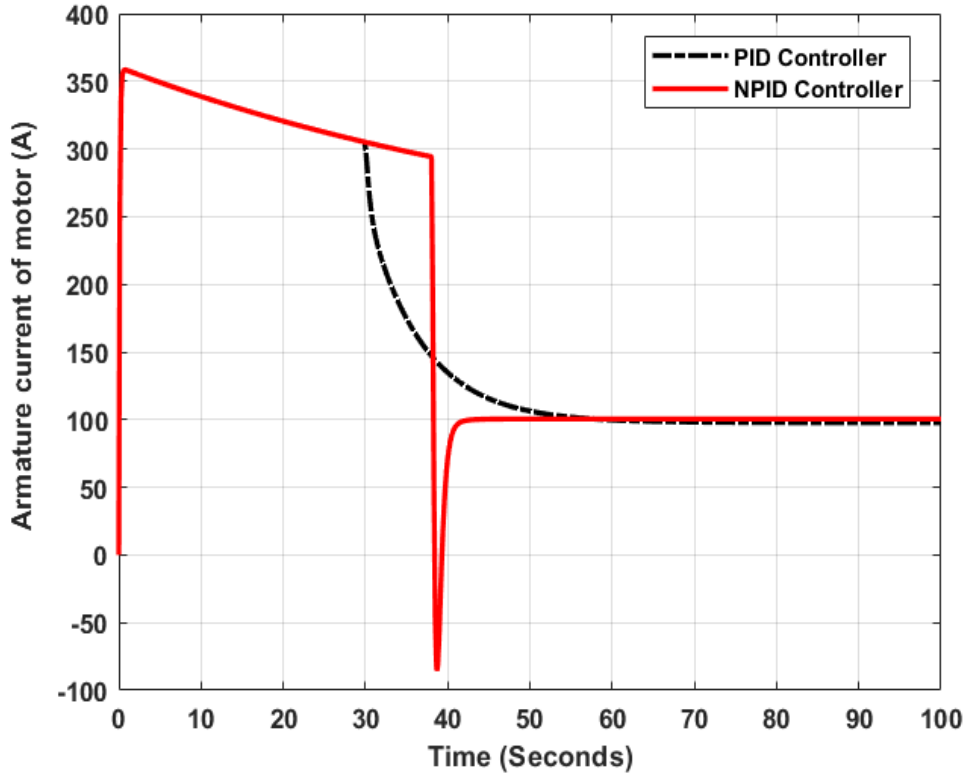

Fig. 10 - The armature current of motor through fixed reference speed.

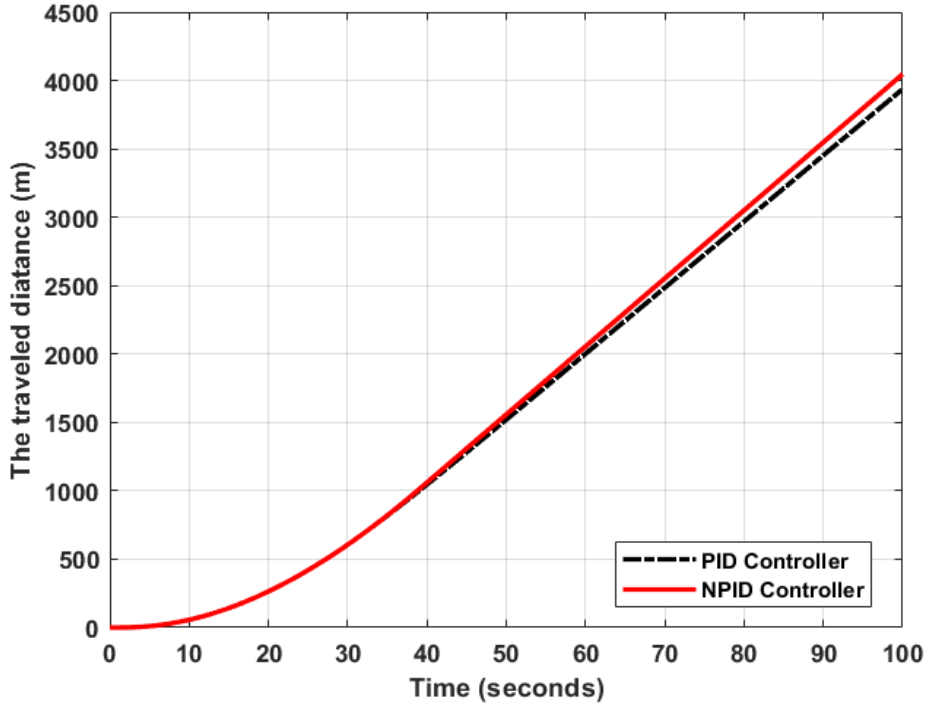

Fig. 11 - The traveled distance through the fixed reference speed test.

In the second test, the driver will change the reference speed continuously. Fig. 12 illustrates the EV velocity response at different commands of reference speed. It is clear that the NPID control can track accurately the reference speed without overshoot and steady-state error. PID control has poor tracking performance (slow response and high steady-state error). Also, Fig. 13 shows the Instantaneous error through the staircase test. It is obvious the NPID can absorb the disturbance caused by the continuous change in operating points. Also, the NPID controller can reduce the root mean square of error by 30.1% compared to the PID controller.

Fig. 14 demonstrates the corresponding armature current of the motor through this test. It is noted that the current increases highly at each change in reference speed. Fig. 15 shows the traveled distance through the different commands of the reference speed test. It is clear that the EV at NPID control moves distance more than the conventional PID control.

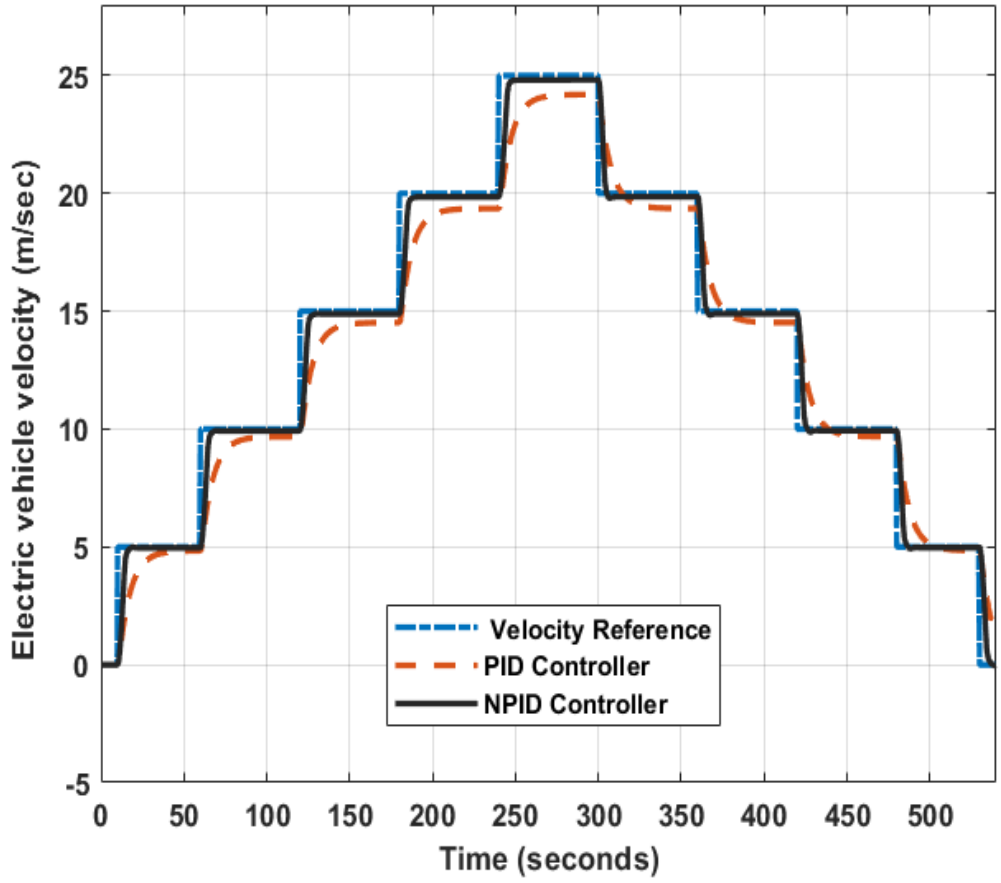

Fig. 12 - The EV velocity response at different commands of reference speed.

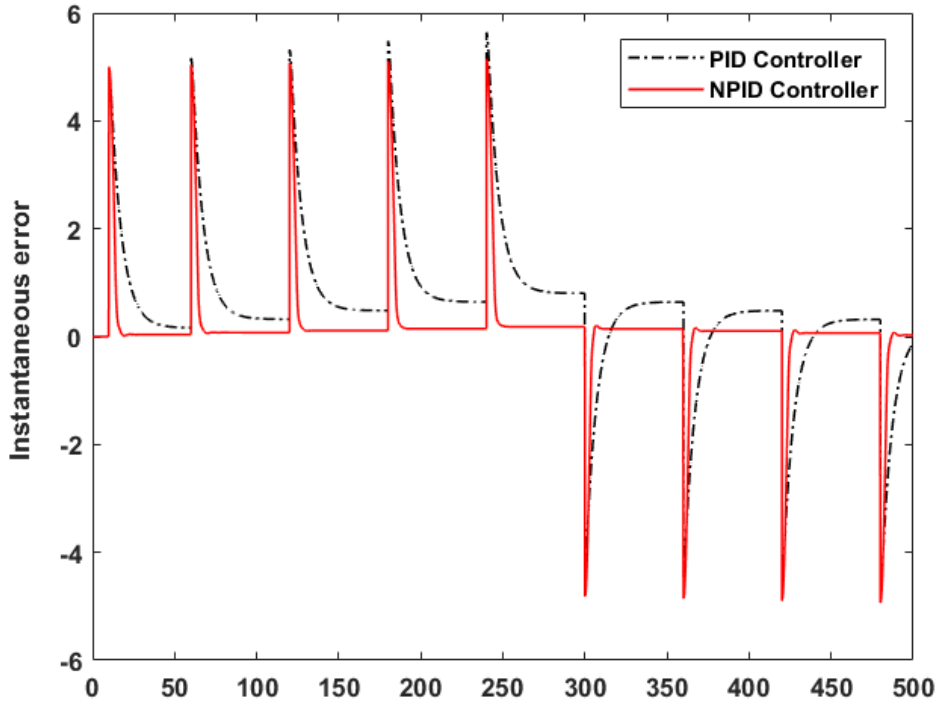

Fig. 13 - Instantaneous error through the staircase test.

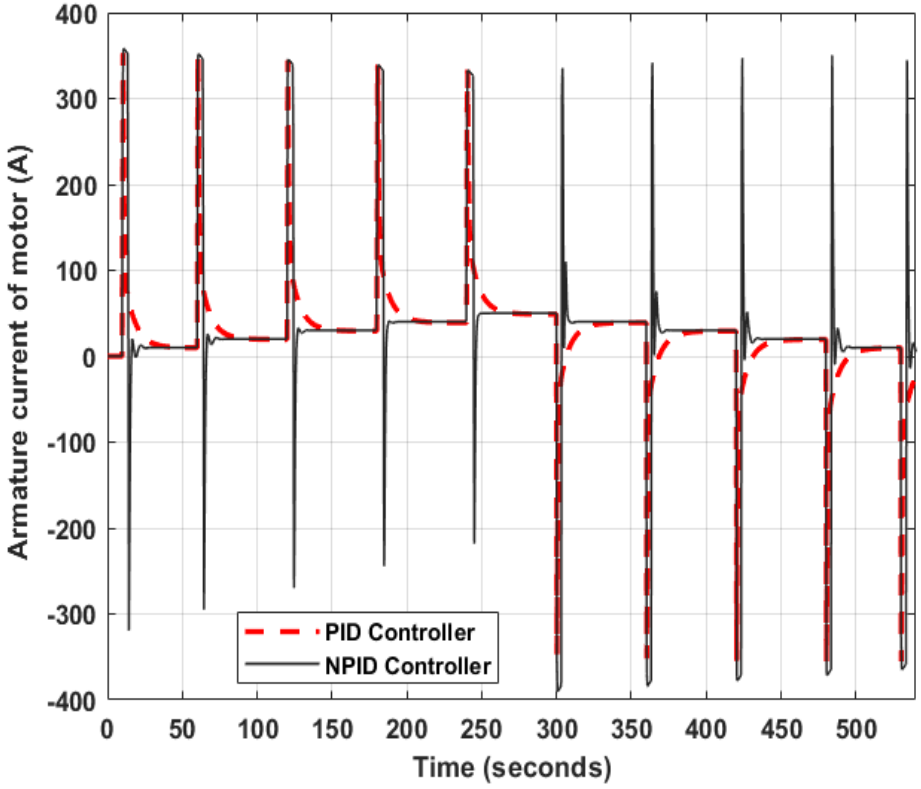

Fig. 14 - The armature current of motor through fixed reference speed.

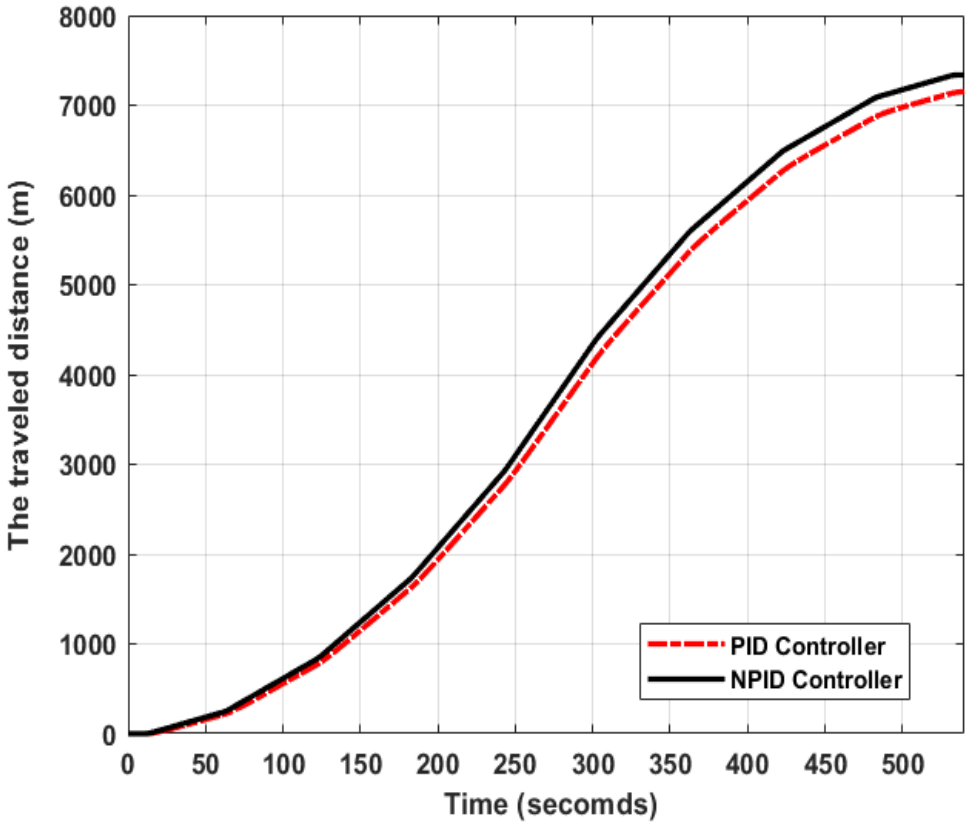

Fig. 15 - The traveled distance through the continuous change of reference speed test.

5. Conclusion

An advanced proposed technique for nonlinear PID control was developed. The main objective of the proposed controller is to follow a preselected reference speed of an electric vehicle (EV). A validated MATLAB/Simulink model was considered. A DC permanent magnet motor with a mechanical transmission was taken into account. Two tests were performed, the first test was realized at fixed reference speed while the second one was applied at various commands of reference speed (Staircase). The simulation results proved that the proposed control technique has promising improved performance compared to conventional PID control. Also, the NPID controller technique can track accurately the reference speed where it has almost zero steady-state error and fine attitude.

References

Abdel Ghany, M.A., M.A. Shamseldin, and A.M. Abdel Ghany. 2017. "A Novel Fuzzy Self Tuning Technique of Single Neuron PID Controller for Brushless DC Motor." International Journal of Power Electronics and Drive Systems 8 (4). https://doi.org/10.11591/ijpeds.v8i4.pp1705-1713.

Aghdam, Mahlagha M., Ricardo P. Aguilera, Li Li, and Jianguo Zhu. 2017. "Fuzzy-Based Self-Tuning Model Predictive Direct Power Control of Grid-Connected Multilevel Converters." 2017 20th International Conference on Electrical Machines and Systems, ICEMS 2017. https://doi.org/10.1109/ICEMS.2017.8056425.

Bingul, Zafer. 2018. "Comparison of PID and FOPID Controllers Tuned by PSO and ABC Algorithms for Unstable and Integrating Systems with Time Delay." Optim Control Appl Meth, no. November 2015. https://doi.org/10.1002/oca.2419.

Dinc, Ali, and Murat Otkur. 2020. "Optimization of Electric Vehicle Battery Size and Reduction Ratio Using Genetic Algorithm." In 2020 11th International Conference on Mechanical and Aerospace Engineering, 281–85. https://doi.org/10.1109/icmae50897.2020.9178899.

Ebrahim, M A, and F Bendary. 2016. "Reduced Size Harmony Search Algorithm for Optimization." Journal of Electrical Engineering, 1–8.

Engineering, Mechanical, and Sciences Issn. 2017. "Second Order Sliding Mode Control for Direct Drive Positioning System." Journal of Mechanical Engineering and Sciences 11 (4): 3206–16.

Franchi, Antonio, and Anthony Mallet. 2017. "Adaptive Closed-Loop Speed Control of BLDC Motors with Applications to Multi-Rotor Aerial Vehicles." In 2017 IEEE International Conference on Robotics and Automation (ICRA) Singapore., 5203–8.

Gaurav, Abhishek, and Anurag Gaur. 2020. "Modelling of Hybrid Electric Vehicle Charger and Study the Simulation Results." In 2020 International Conference on Emerging Frontiers in Electrical and Electronic Technologies (ICEFEET), 1–6. https://doi.org/10.1109/icefeet49149.2020.9187007.

Gong, Yi, Yong Liu, and Zhenmin Tang. 2013. "Path Tracking of Unmanned Vehicle Based on Parameters Self-Tuning Fuzzy Control." 2013 IEEE International Conference on Cyber Technology in Automation, Control and Intelligent Systems, IEEE-CYBER 2013, 52–57. https://doi.org/10.1109/CYBER.2013.6705419.

Hedengren, John. 2007. “Electric Vehicle Model.” 2007. https://www.mathworks.com/matlabcentral/fileexchange/16613-electric-vehicle-model.

Hurtik, Petr, Vojtech Molek, and Jan Hula. 2020. “Data Preprocessing Technique for Neural Networks Based on Image Represented by a Fuzzy Function.” IEEE Transactions on Fuzzy Systems 28 (7): 1195–1204. https://doi.org/10.1109/TFUZZ.2019.2911494.

Moore, Bryan J., Theodore Berger, and Dong Song. 2020. “Validation of a Convolutional Neural Network Model for Spike Transformation Using a Generalized Linear Model.” Proceedings of the Annual International Conference of the IEEE Engineering in Medicine and Biology Society, EMBS 2020-July: 3236–39. https://doi.org/10.1109/EMBC44109.2020.9176458.

Omar, M, M A Ebrahim, A M, and F Bendary. 2016. “Tuning of PID Controller for Load Frequency Control Problem via Harmony Search Algorithm.” Indonesian Journal of Electrical Engineering and Computer Science 1 (2): 255–63. https://doi.org/10.11591/ijeecs.v1i2.pp255-263.

Pathak, Rajeev Ranjan, and Anindiata Sengupta. 2020. “Harmony Search Based Adaptive Sliding Mode Control for Inverted Pendulum.” In 2020 IEEE Calcutta Conference, CALCON 2020 - Proceedings, 171–75. https://doi.org/10.1109/CALCON49167.2020.9106529.

Press, Ieee, Linda Shafer, George W Arnold, and David Jacobson. 2013. ANALYSIS OF ELECTRIC MACHINERY AND DRIVE SYSTEMS. IEEE Press Editorial Board 2013 John Anderson, Editor in Chief Linda.

Rajabi, Nima, and Amir Hossein. 2018. “Sliding Mode Trajectory Tracking Control of a Ball - Screw - Driven Shake Table Based on Online State Estimations Using EKF / UKF.” WILEY, no. November 2017: 1–13. https://doi.org/10.1002/stc.2133.

Ren, Yongping, Zongli Li, and Fan Zhang. 2010. “A New Nonlinear PID Controller and Its Parameter Design.” International Journal of Computer, Electrical, Automation, Control and Information Engineering 4 (12): 1950–55.

Salim, Z, and SCK Junoh. 2017. “Tracking Performance of NPID Controller for Cutting Force Disturbance of Ball Screw Drive NA Anang1, L. Abdullah1, Z. Jamaludin1, TH Chiew1, M. Maharof1.” Jmes.Ump.Edu.My 11 (4): 3227–39. http://jmes.ump.edu.my/images/Volume 11 Issue 4 December 2017/25_Anang et al.pdf.

Scientiarum, Acta. 2017. “DSPACE Real Time Implementation of Fuzzy PID Position Controller for Vertical Rotating Single Link Arm Robot Using Four-Quadrant BLDC Drive,” 301–11. https://doi.org/10.4025/actascitechnol.v39i3.28416.

Shamseldin, M.A., A.A. El-Samahy, and A.M.A. Ghany. 2017. “Different Techniques of Self-Tuning FOPID Control for Brushless DC Motor.” In 2016 18th International Middle-East Power Systems Conference, MEPCON 2016 - Proceedings. https://doi.org/10.1109/MEPCON.2016.7836913.

Shamseldin, M.A., M.A.A. Ghany, and A.M.A. Ghany. 2018. “Performance Study of Enhanced Non-Linear PID Control Applied on Brushless DC Motor.” International Journal of Power Electronics and Drive Systems 9 (2). https://doi.org/10.11591/ijpeds.v9n2.pp536-545.

Shamseldin, Mohamed A., Mohamed Sallam, A. M. Bassiuny, and A. M. Abdel Ghany. 2018. “A Novel Self-Tuning Fractional Order PID Control Based on Optimal Model Reference Adaptive System.” International Journal of Power Electronics and Drive Systems 10 (1): 230–41. https://doi.org/10.11591/ijpeds.v10.i1.

Shamseldin, Mohamed A., Mohamed Sallam, A. M. Bassiuny, and A. M.Abdel Ghany. 2019. “LabVIEW Implementation of an Enhanced Nonlinear PID Controller Based on Harmony Search for One-Stage Servomechanism System.” Journal of Computational and Applied Research in Mechanical Engineering 12: 4161–79. https://doi.org/10.15282/jmes.12.4.2018.13.0359.

Shamseldin, Mohamed A., Mohamed Sallam, A. M. Bassiuny, and A. M.Abdel Ghany. 2019. “A New Model Reference Self-Tuning Fractional Order PD Control for One Stage Servomechanism System.” WSEAS Transactions on Systems and Control 14: 8–18.

Shamseldin, Mohamed A, M Abdullah Eissa, and Adel A El-samahy. 2015. “Practical Implementation of GA-Based PID Controller for Brushless DC Motor.” In 17th International Middle East Power System Conference (MEPCON’15) Mansoura University,Egypt, December 15-17 ,2015.

Siegel, Barry. 2020. “Industrial Anomaly Detection: A Comparison of Unsupervised Neural Network Architectures.” IEEE Sensors Letters 4 (8): 15–18. https://doi.org/10.1109/LSENS.2020.3007880.

Stankovi, Momir R, Milica B Naumović, Stojadin M Manojlović, and Srđan T Mitrović. 2014. “FUZZY MODEL REFERENCE ADAPTIVE CONTROL OF VELOCITY SERVO SYSTEM .” FACTA UNIVERSITATIS Series: Electronics and Energetics 27 (December): 601–11. https://doi.org/10.2298/FUEE1404601S.

Technology, Applied Information. 2015. “THE DESIGN OF THE HYBRID PID-ANFIS CONTROLLER FOR SPEED CONTROL OF BRUSHLESS DC MOTOR.” Journal of Theoretical and Applied Information Technology 71 (3): 367–76.

Upadhya, Anusha. 2017. “Identification of Sliding and Pre-Sliding Regime Frictio n in a Ball Screw Driven System.” In 2017 International Conference on Intelligent Computing, Instrumentation and Control Technologies (ICICICT), 474–77.

Zhao, Wei, and Xuemei Ren. 2016. “Neural Network-Based Tracking and Synchronization Control for Nonlinear Multi-Motor Driving Servomechanism.” Chinese Control Conference, CCC 2016-Augus: 3525–30. https://doi.org/10.1109/ChiCC.2016.7553901.

Zheng, Chunhong, Yuxin Su, and Paolo Mercorelli. 2019. “A Simple Nonlinear PD Control for Faster and High-Precision Positioning of Servomechanisms with Actuator Saturation.” Mechanical Systems and Signal Processing 121: 215–26. https://doi.org/10.1016/j.ymssp.2018.11.017.

Zhu, Yuan, Mingyue Feng, Xiao Wang, and Xinxi Xu. 2012. “RESEARCH ON INTELLIGENT VEHICLE AUTONOMOUS OVERTAKING BASED ON SINGLE NEURON PID CONTROL.” In Proceeding of IEEE CCIS2012, 2–5.